

## EXPERIMENTAL-THEORETICAL INVESTIGATION OF THE HYDROEXPLOSIVE FORMING OF STRUCTURAL SHELLS

V. G. Bazhenov,<sup>1</sup> V. V. Egunov,<sup>1</sup>

UDC 539.3

S. V. Krylov,<sup>1</sup> S. A. Novikov,<sup>2</sup> and Yu. V. Bat'kov<sup>2</sup>

*The paper describes a procedure for numerical modeling of nonlinear axisymmetric processes of hydroexplosive forming in a coupled formulation. Results of numerical solution are compared with experimental data on hydroexplosive loading of circular plates. Good agreement of theoretical and experimental results is obtained.*

Hydroexplosive forming as a method for utilizing explosion energy has been employed to manufacture articles from high-strength materials since the middle of the 1950s. Theoretical foundations of hydroexplosive forming are described in [1–5], whose authors have made a considerable contribution to their development. However, because of the necessity of taking into account many different factors (detonation of explosives, shock wave propagation in a liquid, and high-velocity plastic deformation of bars), existing methods for solving technological problems can give only estimates of the main technological parameters. Analytical methods can be used only under substantial simplifications. Therefore, the only possibility of theoretical analysis for such problems is the employment of numerical methods.

**Formulation of the Problem and Method of Solution.** The problem considered is formulated in a two-dimensional coupled formulation. The dynamic deformation of the bar and its interaction with the liquid and the mold is described using the procedure of [6, 7], which is based on the relations of continuum mechanics. In cylindrical coordinates  $(r, \beta, z)$ , the relationship between the strain rate tensor and displacement rates in the metrics of the current state is given by

$$\begin{aligned} \dot{\epsilon}_{rr} &= \dot{v}_{r,z}/r - \dot{v}_r/r^2, & \dot{\epsilon}_{zz} &= \dot{v}_{z,z}/r, & \dot{\epsilon}_{\beta\beta} &= \dot{v}_r/r^2, \\ \dot{\epsilon}_{rz} &= (\dot{v}_{r,z}/r + \dot{v}_{z,r}/r - \dot{v}_z/r^2)/2, \end{aligned}$$

where  $\dot{v}_\alpha = r\dot{u}_\alpha$  ( $\alpha = r, z$ ) and  $\dot{u}_\alpha$  are the components of the displacement velocity vector. The subscript after comma denotes differentiation with respect to the corresponding variable and the dot above denotes partial derivative with respect to time.

The variational equation of motion is written in cylindrical coordinates in the form of Jourdain's equation

$$\begin{aligned} \iint_{\Omega} \left[ \sigma_{rr} \delta \dot{v}_{r,r} + \sigma_{zz} \delta \dot{v}_{z,z} + \sigma_{rz} (\delta \dot{v}_{r,z} + \delta \dot{v}_{z,r}) - \frac{\sigma_{rr} - \sigma_{\beta\beta}}{r} \delta \dot{v}_r - \frac{\sigma_{rz}}{r} \delta \dot{v}_z + \rho (\ddot{u}_r \delta \dot{v}_r + \ddot{u}_z \delta \dot{v}_z) \right] d\Omega \\ - \int_{G_p} (p_r \delta \dot{v}_r + p_z \delta \dot{v}_z) ds - \int_{G_q} (q_r \delta \dot{v}_r + q_z \delta \dot{v}_z) ds = 0. \end{aligned} \quad (1)$$

Here  $\sigma_{ij}$  [ $i, j = (r, \beta, z)$ ] are the stress tensor components,  $p_\alpha$  and  $q_\alpha$  are the components of the surface load and contact pressure, and  $\rho$  is the density.

---

<sup>1</sup>Institute of Mechanics, Nizhniy Novgorod State University, Nizhniy Novgorod 603950. <sup>2</sup>Institute of Experimental Physics, Sarov 607190. Translated from *Prikladnaya Mekhanika i Tekhnicheskaya Fizika*, Vol. 43, No. 5, pp. 176–181, September–October, 2002. Original article submitted December 18, 2000; revision submitted March 12, 2001.

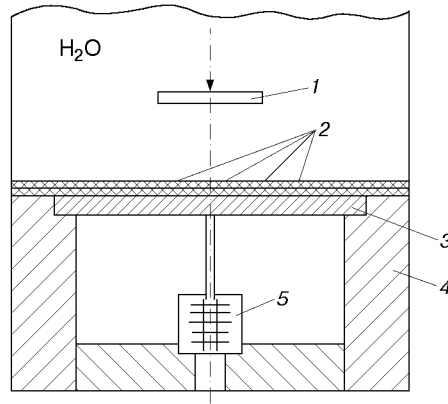


Fig. 1

Equation (1) is supplemented by the corresponding initial and kinematic boundary conditions. The elastoplastic deformation of the bar is described by the plastic flow equations with linear kinematic hardening.

The problem is solved by the variational-difference method using an explicit “cross”-type scheme [7]. Large strains and distortion are taken into account by stepwise rearrangement of the geometry of the bar in Eulerian cylindrical coordinates. Discontinuous solutions are calculated using a smoothing apparatus based on the use of conservative artificial viscosity [8].

The dynamics of the liquid and detonation products are described using laws of conservation of mass, momentum, and energy written in the form of Euler’s laws [9]:

$$\int_{\Omega} \left( \frac{\partial \rho}{\partial t} + \operatorname{div} \rho \mathbf{v} \right) d\Omega = 0,$$

$$\int_{\Omega} \left( \frac{\partial(\rho \mathbf{v})}{\partial t} + \operatorname{div}[p \mathbf{n} + (\mathbf{v}, \mathbf{n}) \rho \mathbf{v}] \right) d\Omega = 0, \quad \int_{\Omega} \left( \frac{\partial e}{\partial t} + \operatorname{div}(e + p) \mathbf{v} \right) d\Omega = 0.$$

Here  $p$  is the pressure,  $\mathbf{v}$  is the velocity vector,  $\mathbf{n}$  is the outward normal vector, and  $e$  is the internal energy.

The equation of state is written as

$$e = [p + fB(1 - \rho/\rho_0)]/[\rho(f - 1)],$$

where  $f$ ,  $B$ , and  $\rho_0$  are constants. The system of equations is integrated numerically using a modified Godunov’s scheme [10], which has the second order of accuracy on smooth solutions and monotonic behavior on discontinuities.

Detonation of an explosive charge is modeled using a radial model of detonation. According to this scheme, each point of the explosive reached by a detonation wave issuing from a specified region of initiation, becomes a source of detonation and radiates a detonation wave. According to the hydrodynamic theory of detonation, the speed of propagation of a detonation wave ( $D$ ) is constant and is linked to the calorific value  $Q$  of the explosive by the relation  $D^2 = 2(\gamma^2 - 1)Q$  ( $\gamma$  is the adiabatic exponent of detonation products). Thus, detonation propagates radially from the point of initiation. The energy release due to chemical reactions is taken into account by increasing the internal energy  $e$  by a value corresponding to the calorific value  $Q$  in computation cells through which the detonation wave front propagates.

The conditions on the surfaces of contact of the liquid with the plate are formulated as nonpenetration conditions on the surface segments in contact at the given moment and the free-boundary conditions on the remaining segments. The criterion for transition from the nonpenetration conditions to the conditions on the free boundary resulting from rupture is the satisfaction of the inequality  $q < q_k$  ( $q$  is the contact pressure and  $q_k = 0$  is a constant that describes the rupture strength of the liquid). The contact criterion is the intersection of the surfaces of the interacting objects.

**Experimental Procedure.** To verify the numerical results, we performed experiments on hydroexplosive loading of circular plates. The experimental setup is shown schematically in Fig. 1. An explosive charge 1 weighing 48 g was placed in a polyethylene bag containing water at 30 mm from a circular plate (bar) 3 made of Kh18N10T steel (diameter 155 mm and thickness 6 mm), which, in turn, was placed in a supporting cylinder 4.

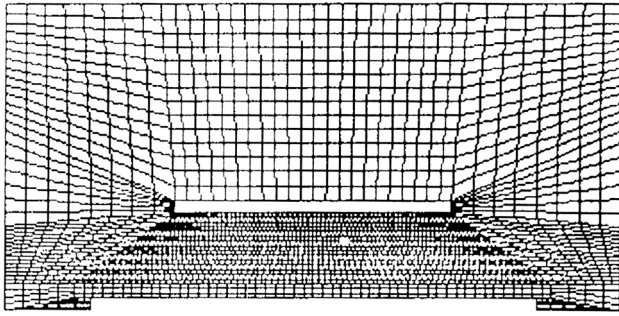


Fig. 2

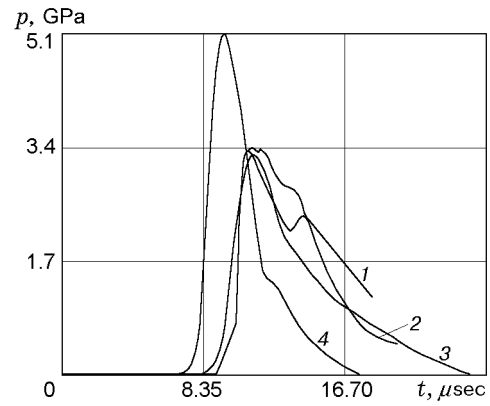


Fig. 3

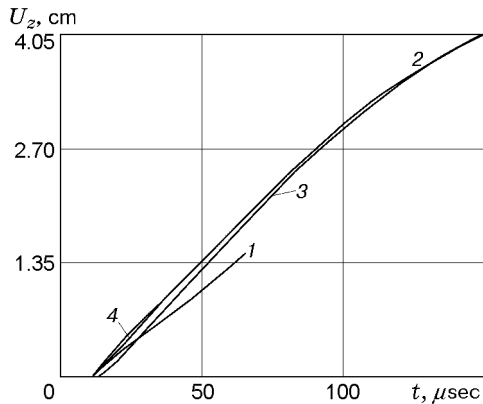


Fig. 4

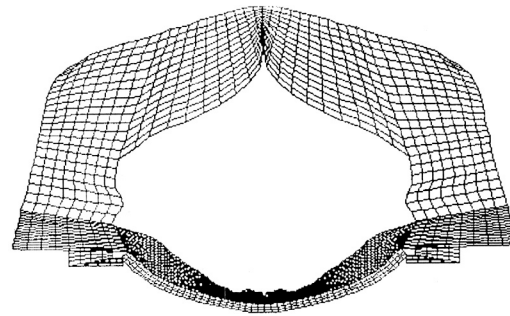


Fig. 5

Measurements of the pressure acting on the bar and the displacement of its central zone (pole) were conducted. The pressure was measured by Manganin gauges. The measuring technique using these gauges is described in [11]. Four DM-50 type Manganin gauges 2 in the shape of a  $6 \times 7$  mm plane rectangular grid made from a PÉMS Manganin wire of 0.05 mm diameter were arranged as follows: one was located at the center of the plate, two were placed at 30 mm from the center of the plate, and one was placed at 50 mm from the center of the plate. The gauges were isolated from the steel plate by a fluoroplastic film 0.2 mm thick. The change in the resistance of the gauges was recorded by a bridge circuit using a PIID-4 device and an OK-33 cathode oscilloscope. The sensitivity of the measuring channel was not less than 2 V/GPa, and the measurement error of the pressure amplitude is not more than 10%.

The displacement of the plate was measured by an electrocontact gauge 5. The contacts in the gauge were made from a brass foil 0.05 mm thick. The gauge rod was mounted closely to the plate. During motion of the plate, the working contacts are closed in series by the rod needle, which shapes electric pulses on the special  $RC$ -chains of the signal shaper. The pulses were recorded by an SVR raster sweep oscillographs.

Before the beginning of the experiment, concentric circles were drawn on the bar. Measurements of the radii of these circles after termination of the experiment gave the distribution of the hoop strains  $\varepsilon_\theta$  on one of the surfaces of the bar. Simultaneously, we measured the thickness of the bar at various points.

**Comparison of Calculations and Experimental Results.** The computational region was covered with a grid of tetragonal elements (Fig. 2), whose number was as follows: 150 for the bar, 280 for the explosive charge, 952 for the region occupied by water, and 32 for the supporting ring. The mechanical characteristics of the plate material and supporting ring were as follows:  $E = 2 \cdot 10^5$  MPa,  $\nu = 0.3$ ,  $\rho = 7.8$  g/cm<sup>3</sup>,  $\sigma_{\text{yield}} = 230$  MPa, and hardening modulus  $g = 830$  MPa. The constants included in the equation of state for water were as follows:  $\rho_0 = 1$  g/cm<sup>3</sup>,  $B = 304.5$  MPa, and  $f = 7.15$ . In the calculation of the detonation process, we used the following values:  $D = 8.75$  km/sec,  $Q = 5300$  J/g,  $\gamma = 1.25 + 1.51\rho/\rho_0$ ,  $\rho_0 = 1.55$  g/cm<sup>3</sup>.

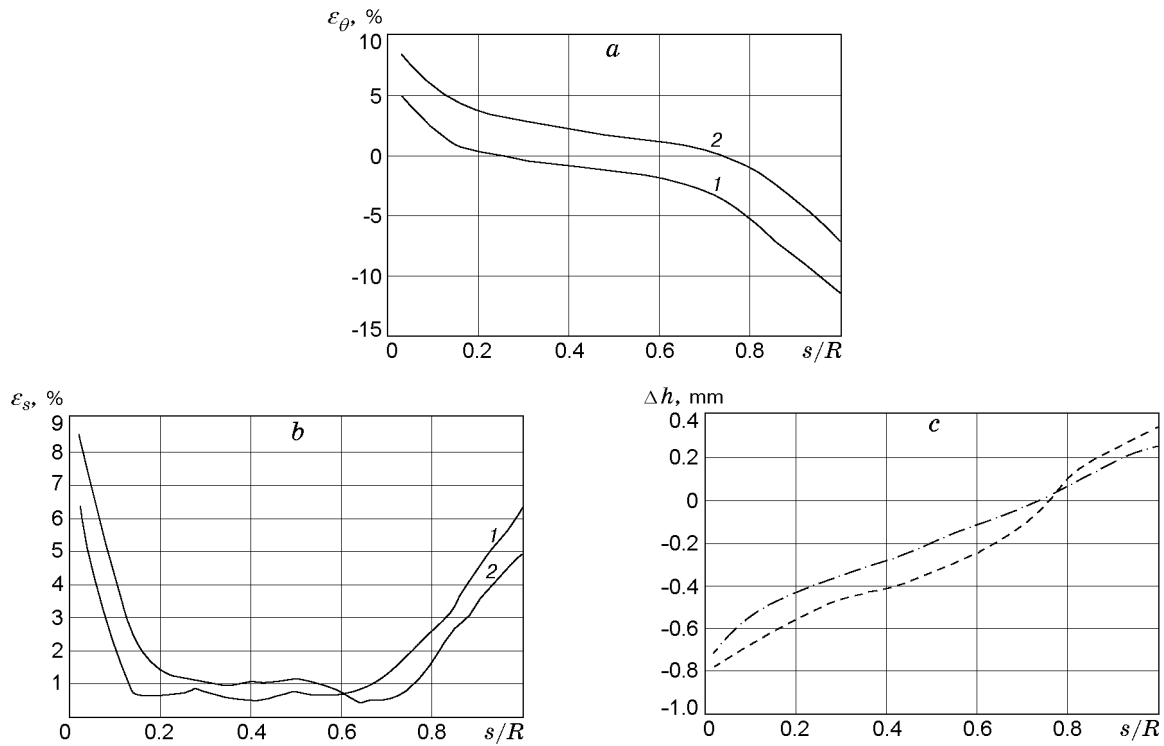


Fig. 6

The calculation and experimental results are given in Figs. 3–6. Figure 3 shows curves of the pressure  $p(t)$  acting at the center of the bar (curves 1 and 2 are experimental data obtained in two identical experiments, and curves 3 and 4 are predicted data obtained for the radial model and the model of “instantaneous” detonation, respectively). Figure 4 gives experimental and calculated curves of the displacement of the central point of the bar  $U_z(t)$  (notation same as in Fig. 3). The computational region at the final stage of deformation is shown in Fig. 5.

The forming process can be conditionally divided into several stages. At the first stage there is detonation of the explosive and its transformation into expanding detonation products. The second stage involves the propagation of shock waves in the liquid surrounding the explosive and interaction of them with the bar. The amplitude of the pressure acting in the central zone of the bar reaches 3.4 GPa, and the pulse duration is approximately 15  $\mu\text{sec}$ . The radial model gave a curve of  $p(t)$  that is in good agreement with experimental data. In the case where the dimensions of the explosive charge are comparable with the distance to the bar, the simpler model of “instantaneous” detonation leads to considerable errors in determining the amplitude of the pressure acting on the bar (see Fig. 3).

The third stage involves intense dynamic deformation of the bar, its separation from the liquid (at  $t \approx 25 \mu\text{m}$ ), and motion by inertia. The deformation process is completed by the time  $t \approx 160 \mu\text{sec}$ . In the calculations, the maximum deflection was 43 mm (see Fig. 4). Measurements of the bar after the experiment showed that the maximum deflection was 48 mm. Calculated curves of the displacement of the central zone of the bar obtained for the model of “instantaneous” detonation and the radial model practically coincide. This is due to the fact that the pressure pulses acting on the bar differ only slightly.

Figure 6a and b gives curves of hoop ( $\varepsilon_\theta$ ) and meridional ( $\varepsilon_s$ ) strains plotted on the inner (curves 1) and outer (curves 2) surfaces of the bar, respectively. Figure 6c shows curves of the variation of the thickness of the bar  $\Delta h$  (dashed curve refer to the experiment and the dot-and-dashed curve refer to the calculation). Here  $s/R$  is the dimensionless length of the arc reckoned from the symmetry axis of the bar.

From the calculations it follows that the stress–strain state is nearly non-momentum. Maximum strains occur near the edge and the symmetry axes. Furthermore, the hoop strains are alternating (compressing in a zone adjacent to the edge of the bar and expanding near the symmetry axis), and the meridional strains are positive everywhere. The variation in the thickness of the bar is nonuniform. In a region of approximate dimension  $0.3R$  adjacent to the bar edge, the thickness increases, which is due to considerable compressing hoop strains in it. The thicknesses of the bar measured at ten points on the generatrix after the experiment agree well with the corresponding calculated values.

**Conclusions.** A procedure of mathematical modelling of hydroexplosive forming is developed and implemented using the “Dinamika-2” program complex [12]. Good agreement between numerical and experimental results for the main loading and deformation parameters makes it possible to recommend this procedure for designing the technological processes involved in hydroexplosive forming.

## REFERENCES

1. R. V. Pikhtovnikov and V. I. Zav'yalova, *Explosive Forming of Sheet Metal* [in Russian], Mashinostroenie, Moscow (1964).
2. V. G. Stepanov and I. A. Shavrov, *Impulsive Metal Working in Marine Engineering* [in Russian], Sudostroenie, Leningrad (1968).
3. V. K. Borisevich, “General approach to determining external loading parameters in explosive forming,” in: *Metal Working by Pulsed Pressure* [in Russian], Mashinostroenie, Moscow (1977), pp. 14–25.
4. V. K. Borisevich, V. P. Sabel'kin, and S. N. Solodyankin, “Numerical simulation on a computer of the process of explosive forming,” *J. Appl. Mech. Tech. Phys.*, No. 2, 249–256 (1979).
5. M. A. Anuchin (ed.), *Explosive Forming. Theoretical Foundations* [in Russian], Mashinostroenie, Moscow (1972).
6. V. G. Bazhenov, S. V. Zefirov, and I. N. Tsvetkova, “Numerical modeling of problems of unsteady contact interaction of structures under deformation,” in: *Applied Problems of Strength and Plasticity. Numerical Modeling of Physicomechanical Processes* (collected scientific papers) [in Russian], No. 52, Izd. Nizhegorod. Univ., Nizhnii Novgorod (1995), pp. 154–160.
7. V. G. Bazhenov, S. V. Zefirov, and A. I. Kibets, “Numerical implementation the variational-difference momentum scheme for solving nonlinear problems of dynamics of thick shells under pulsed actions,” in: *Applied Problems of Strength and Plasticity. Methods of Solution* (collected scientific papers) [in Russian], No. 38, Izd. Gor'k. Univ., Gor'kii (1988), pp. 66–73.
8. V. G. Bazhenov and S. V. Zefirov, “Conservative smoothing of discontinuous stress waves in finite-element method,” *Vestn. Nizhegorod. Univ., Ser. Mekh.*, No. 1, 166–173 (2001).
9. S. K. Godunov (ed.), *Numerical Solution of Multidimensional Problems of Gas Dynamics* [in Russian], Nauka, Moscow (1976).
10. M. Kh. Abuzyarov, V. G. Bazhenov, and A. V. Kochetkov, “New effective method for increasing the accuracy of Godunov's scheme,” in: *Applied Problems of Strength and Plasticity. Methods of Solution* (collected scientific papers) [in Russian], No. 35, Izd. Gor'k. Univ., Gor'kii (1987), pp. 44–50.
11. Yu. V. Bat'kov, S. A. Novikov, A. P. Pogorelov, and V. A. Sinitsyn, “Investigation of the process of explosive transformation of composite 50/50 TNT/RDX behind a nonstationary shock front,” *Combust. Expl. Shock Waves*, **15**, No. 5, 676–678 (1979).
12. V. G. Bazhenov, S. V. Zefirov, A. V. Kochetkov, et al., “‘Dinamika-2’ program complex,” in: *Program Systems* (collected scientific papers) [in Russian], Tomsk Polytech. Inst., Tomsk (1999), pp. 40–45.